Full-Wave Modeling of Generalized Double Ridge Waveguide T-Junctions

Chi Wang, *Student Member, IEEE*, and Kawthar A. Zaki, *Fellow, IEEE*

***Abstract*— A rigorous technique for full wave modeling of the generalized double ridge waveguide T-junction has been developed. Eigen modes in each ridge waveguide region are obtained using mode-matching technique. Based on the eigen mode expansion method, combining the cascading procedure and computation of the magnetic fields of each mode at the shorted ports, the generalized admittance matrices and scattering matrices of all three ports are obtained. The method is general and very efficient. The accuracy and versatility of the method are verified through several numerical examples. The computed dominant mode's S-parameters are compared with that by finite element method (HFSS) and shown to be in good agreement.**

I. Introduction

WAVEGUIDE T-junctions are important components in modern communication systems and many other microwave applications [1], [2]. With the rapid development of technology, the requirement for high performance, wide band, small size T-junctions is increasing. Because ridge waveguides have low cutoff frequency and wide bandwidth [3]–[6], broad band ridge waveguide T-junctions are the ideal components for the applications [11], [12]. To design systems employing ridge waveguide T-junctions, accurate and efficient computer aided design tool for computing the generalized scattering matrices is essential.

A few numerical techniques have been developed in the past several decades. Although purely numerical methods such as finite element method are versatile to the structure, the efficiency and memory requirement usually make them not suitable for optimization, furthermore, purely numerical methods cannot conveniently provide generalized scattering matrices including the effects of the higher order modes. Mode-matching method based on field expansion into cavity waves and matching the boundary at the port can compute the generalized scattering matrix of the rectangular waveguide T-junction efficiently [8]. By combining the scattering matrices of the symmetrical waveguide T-junction with the scattering matrices of the waveguide discontinuity, the total scattering matrices of waveguide T-junction of different cross sections can be obtained [9]. To avoid numerical instabilities caused by the large attenuation constant of the cut-off modes, a modification of the mode matching method is developed, which effectively allows the generalized scattering matrix computation at a central reference plane.

Manuscript received March 29, 1996.
The authors are with the Department of Electrical Engineering, University of Maryland, College Park, MD 20742 USA.
Publisher Item Identifier S 0018-9480(96)08552-3.

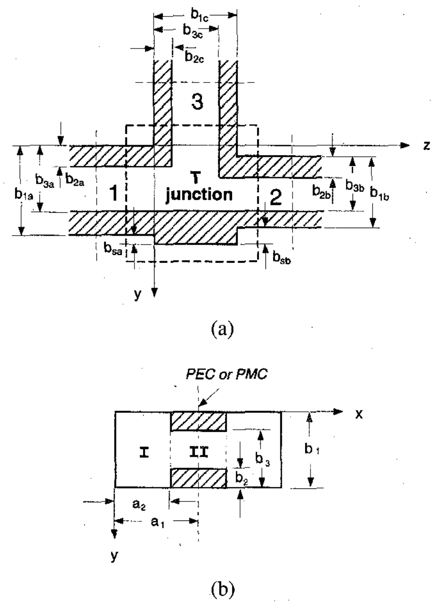

Fig. 1. Generalized double ridge T-junction. (a) Sectional side view of the T-junction. (b) Typical cross section of each arm.

Recently, three plane mode-matching technique (TPMMT) [10] and equivalent methods [13] were proposed for solving the multiport microwave network problems. Coaxial probe in rectangular waveguide and all ridge waveguide T-junction were reported to be studied by the method [12], [14], [15]. Although three plane mode-matching technique can simplify and solve the complicated T-junction problem, one can not obtain the generalized scattering matrices of the T-junction for all three ports. The purpose of this paper is to describe a new method which can overcome the limitations of the above methods and suitable to general structures.

In this paper, a rigorous technique based on new application of the eigen mode expansion method [7] and combining the cascading procedure [16] is introduced to model the generalized double ridge waveguide T-junctions shown in Fig. 1. The generalized admittance and scattering matrices including all the higher order modes in all ridge waveguide ports are obtained. Instead of computing the admittance matrices directly from the fields of the T-junction, generalized scattering matrices and the field coefficients in each waveguide region in the T-junction are used to obtain the subadmittance matrices. The generalized scattering matrices of the T-junction are then obtained from the admittance matrix. The method preserves numerical accuracy and accepts arbitrary cross section of all ports. The method is general, very efficient, and can be used to solve other complicated multiport network problems. The accuracy and versatility of the method are verified through several numerical examples. The computed dominant mode's S-parameters are compared with that by finite element method using HFSS and shown in good agreement.

II. Fundamental Theory

The electromagnetic field in a waveguide can be expressed as superposition of incident and reflected waves of all the eigenmodes. For TE and TM modes existing in a waveguide with uniform cross section normal to the z direction, the total electromagnetic fields can be expressed as

$$\begin{aligned}\vec{E}(x,y,z) &= \vec{E}_t(x,y,z) + E_z(x,y,z)\hat{z}\\ &= \sum_{i=1}^{N^h} (a_i^h e^{-\gamma_i^h z} + b_i^h e^{\gamma_i^h z})\vec{e}_{ti}^{\,h}(x,y)\\ &\quad + \sum_{i=1}^{N^e} (a_i^e e^{-\gamma_i^e z} + b_i^e e^{\gamma_i^e z})\vec{e}_{ti}^{\,e}(x,y)\\ &\quad + \sum_{i=1}^{N^e} (a_i^e e^{-\gamma_i^e z} - b_i^e e^{\gamma_i^e z})e_{zi}^e(x,y)\hat{z} \quad (1a)\end{aligned}$$

$$\begin{aligned}\vec{H}(x,y,z) &= \vec{H}_t(x,y,z) + H_z(x,y,z)\hat{z}\\ &= \sum_{i=1}^{N^h} (a_i^h e^{-\gamma_i^h z} - b_i^h e^{\gamma_i^h z})\vec{h}_{ti}^{\,h}(x,y)\\ &\quad + \sum_{i=1}^{N^e} (a_i^e e^{-\gamma_i^e z} - b_i^e e^{\gamma_i^e z})\vec{h}_{ti}^{\,e}(x,y)\\ &\quad + \sum_{i=1}^{N^h} (a_i^h e^{-\gamma_i^h z} + b_i^h e^{\gamma_i^h z})h_{zi}^h(x,y)\hat{z} \quad (1b)\end{aligned}$$

$$\gamma_i^{2q} = k_{ci}^{2q} - k_0^2\epsilon_r, q = e,h \quad (1c)$$

where $\vec{e}_{ti}^{\,h}$, $\vec{h}_{ti}^{\,h}$, and h_{zi}^h are the tangential and normal fields of ith TE mode (with propagation constant γ_i^h). $\vec{e}_{ti}^{\,e}$, $\vec{h}_{ti}^{\,e}$, and e_{zi}^e are the tangential and normal fields of ith TM mode (with propagation constant γ_i^e), respectively. $k_{ci}^q, (q = e,h)$ is the cutoff wavenumber of the ridge waveguide's eigenmode. The waveguide eigenmode functions are orthogonal to each other.

By defining the equivalent voltage $v(z)$ and current $i(z)$ of the waveguide mode as [7], [8]

$$v_i^q(z) = a_i^q e^{-\gamma_i z} + b_i^q e^{\gamma_i z} \quad (2a)$$

$$i_i^q(z) = a_i^q e^{-\gamma_i z} - b_i^q e^{\gamma_i z} \quad (2b)$$

$$q = e,h$$

the electromagnetic fields can then be expressed in terms of the equivalent voltage and current as

$$\begin{aligned}\vec{\boldsymbol{E}}(x,y,z) &= \sum_{i=1}^{N^h} v_i^h(z)\vec{e}_{ti}^{\,h}(x,y) + \sum_{i=1}^{N^e} v_i^e(z)\vec{e}_{ti}^{\,e}(x,y)\\ &\quad + \sum_{i=1}^{N^e} i_i^e(z)e_{zi}^e(x,y)\hat{z} \quad (3a)\end{aligned}$$

$$\begin{aligned}\vec{\boldsymbol{H}}(x,y,z) &= \sum_{i=1}^{N^h} i_i^h(z)\vec{h}_{ti}^{\,h}(x,y) + \sum_{i=1}^{N^e} i_i^e(z)\vec{h}_{ti}^{\,e}(x,y)\\ &\quad + \sum_{i=1}^{N^e} v_i^h(z)h_{zi}^h(x,y)\hat{z}. \quad (3b)\end{aligned}$$

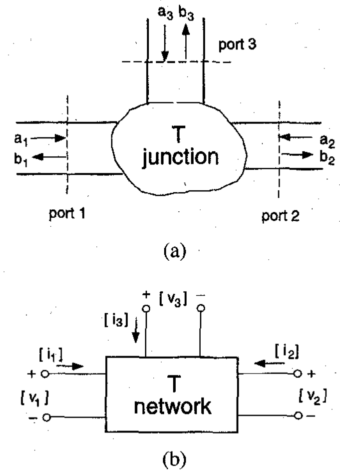

Fig. 2. (a) A generalized T-junction with incident and scattering waves at the ports. (b) Equivalent network of the T-junction with the effects of higher order modes.

Using equivalent circuit concepts [8], the T-junction problem involving discontinuities as shown in Fig. 2, can be solved by computing the admittance matrices of the network as

$$\begin{bmatrix}[i_1]\\ [i_2]\\ [i_3]\end{bmatrix} = \begin{bmatrix}[Y_{11}] & [Y_{12}] & [Y_{13}]\\ [Y_{21}] & [Y_{22}] & [Y_{23}]\\ [Y_{31}] & [Y_{32}] & [Y_{33}]\end{bmatrix}\begin{bmatrix}[v_1]\\ [v_2]\\ [v_3]\end{bmatrix} = [Y]\begin{bmatrix}[v_1]\\ [v_2]\\ [v_3]\end{bmatrix}. \quad (4)$$

One way to compute the subadmittance matrix is by assuming an incident mode field in a port while other two ports are shorted, then computing the tangential magnetic field excited at each port as

$$Y_{ij}^{qp} = \pm \int_{s_p} \vec{\boldsymbol{H}}_{ti}^q \cdot \vec{\boldsymbol{h}}_{tj}^p \, ds_p \quad (5)$$

where $\vec{\boldsymbol{H}}_{ti}^q$ is the tangential magnetic field of ith mode at port p excited by incident fields at port q, $\vec{\boldsymbol{h}}_{tj}^p$ is the tangential magnetic field of jth mode at port $p, (p,q = 1,2,3)$. The sign of the admittance is determined by the direction of the positive power flow and the coordinate system [8], [9].

Another way to obtain the subadmittance matrix is from the relationships between the scattering matrix and the admittance matrix as

$$[S] = [[U] + [Y]]^{-1}[[U] - [Y]] \quad (6a)$$

$$[Y] = [[U] - [S]][[U] + [S]]^{-1} \quad (6b)$$

where $[U]$ is the unit matrix.

III. Description of the Method

The double ridge waveguide T-junction under consideration is shown in Fig. 1. The cross sections of the ridge waveguides are symmetric as shown in Fig. 1(b). By putting a perfect electric conductor (PEC) or a perfect magnetic conductor (PMC)

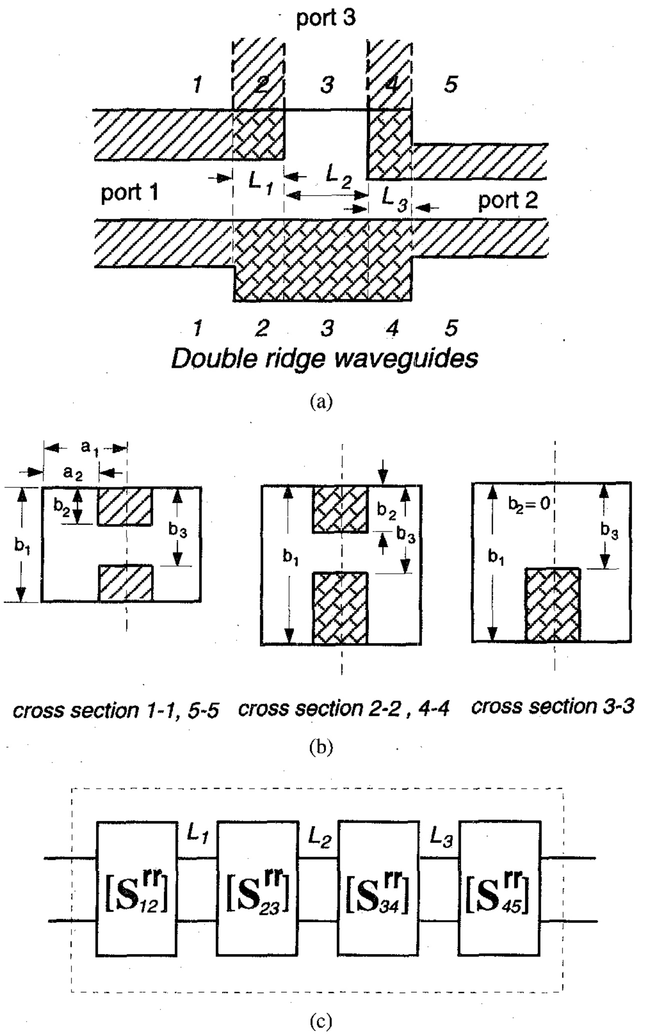

Fig. 3. (a) Side view of the perpendicular arm shorted double ridge T-junction. (b) Cross sections of port 1, and equivalent ridge waveguides. (c) Network representation of the double ridge T-junction when port 3 is shorted.

at the symmetrical planes, only half structure needs to be considered. Several ridge waveguides and their discontinuities exist in the T-junction.

From the previous analysis, it is clear that complete characterization of the T-junction is reduced to the problem of computing the admittance matrix. As the fields of the cut-off modes vary exponentially along the normal direction, numerical instability is introduced when discontinuity exists in the T-junction by the numerical error. Although all the ports except incident port are shorted, because discontinuity exits in the T-junction, the principle of expansion of electromagnetic fields in cavities [8] can not be used to compute the admittance matrices. Instead, generalized scattering matrices of the two-port network combining the field coefficients and a new kind of inner product are used to obtain the admittance matrix to preserve the numerical stability and accuracy of the results.

A. Computation of Admittance Matrices $[Y_{11}]$, $[Y_{12}]$, $[Y_{21}]$, *and* $[Y_{22}]$

When the perpendicular port (port 3 in Fig. 1) is shorted, the resulting structure reduces to a two-port network which can be treated as several ridge waveguides with certain lengths connected together as shown in Fig. 3. A full wave mode-matching technique is used to obtain the generalized scattering matrices of the discontinuities. Therefore the S-matrices of the whole two-port network can be computed by successive cascading of the generalized S-matrices $[S^{rr}_{ij}]$ of the discontinuities between ridge waveguides separated by ridge waveguide of lengths L_i as shown in Fig. 3, as [16]

$$\begin{bmatrix}\boldsymbol{b}_1\\\boldsymbol{b}_2\end{bmatrix}=\begin{bmatrix}[S_{11}] & [S_{12}]\\ [S_{21}] & [S_{22}]\end{bmatrix}\begin{bmatrix}\boldsymbol{a}_1\\\boldsymbol{a}_2\end{bmatrix}=[S]\begin{bmatrix}\boldsymbol{a}_1\\\boldsymbol{a}_2\end{bmatrix}. \quad (7)$$

As the subadmittance matrices $[Y_{11}]$, $[Y_{12}]$, $[Y_{21}]$, and $[Y_{22}]$ of the two-port network are identical to that of the three-port T-junction, instead of computing the tangential magnetic fields at port 1 and port 2 by repeatly shorting port 1 and port 2, they can be obtained easily from the generalized S-matrices of the two-port network using (6b). Obviously, the magnetic fields existing at the short circuited port 3 are available from mode matching expansion coefficients. These fields will be used latter to compute $[Y_{31}]$ and $[Y_{32}]$.

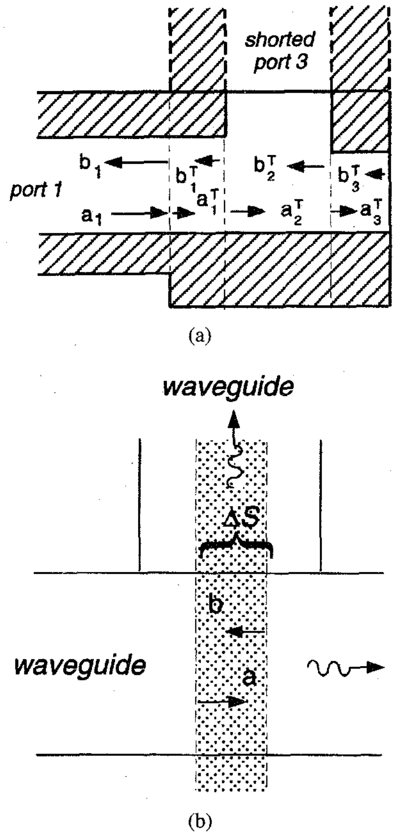

Fig. 4. (a) EM waves in each equivalent ridge waveguide region of the T-junction with port 2 and port 3 shorted. (b) Configuration of partial vertical inner product.

B. Admittance Matrices $[Y_{31}]$ *and* $[Y_{32}]$

To compute the admittance matrix $[Y_{31}]$ or $[Y_{32}]$, all the ports, except incident port have to be shorted. Magnetic field at the surface of the shorted port 3 of the one port network excited by the fields from port 1 needs to be computed in terms of the modal fields of the waveguide port 3. The generalized

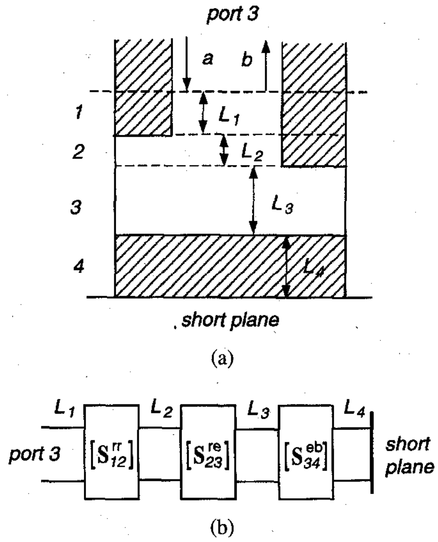

Fig. 5. (a) Side view of the T-junction when port 1 and port 2 shorted. (b) Imaginary two-port network with one port shorted.

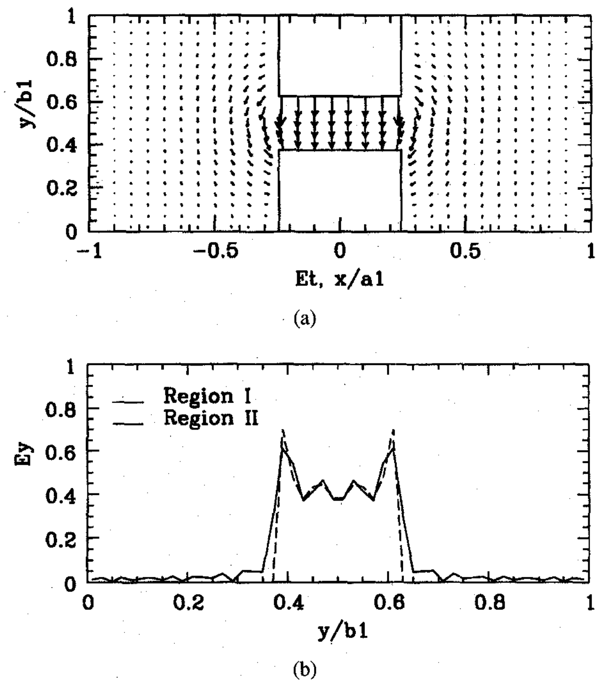

Fig. 6. Field distribution obtained from mode matching with $a_1 = 0.45'', a_2 = 0.34'', b_1 = 0.40'', b_2 = 0.15'', b_3 = 0.25''$. (a) 2-D tangential field plot. (b) E_y at boundary between region I and region II.

scattering matrices of each discontinuity and the total two-port network obtained in part A above can be used to get the generalized scattering matrices related to the field coefficients of port 1 and port 2 which are defined and shown in Fig. 4(a) as

$$\begin{bmatrix}[b_1]\\ [a_i^T]\end{bmatrix} = [S^{1-i}]\begin{bmatrix}[a_1]\\ [b_i^T]\end{bmatrix} \qquad (i = 1, 2, 3) \tag{8a}$$

$$\begin{bmatrix}[b_i^T]\\ [b_2]\end{bmatrix} = [S^{i-2}]\begin{bmatrix}[a_i^T]\\ [a_2]\end{bmatrix} \qquad (i = 1, 2, 3). \tag{8b}$$

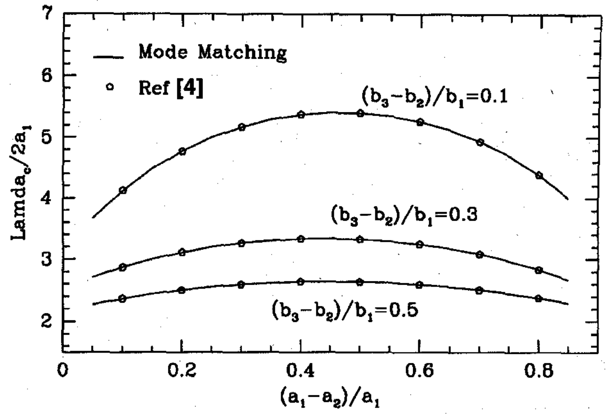

Fig. 7. Cutoff wavelength of a double ridge waveguide with respect ratio $b_1/a_1 = 0.5$.

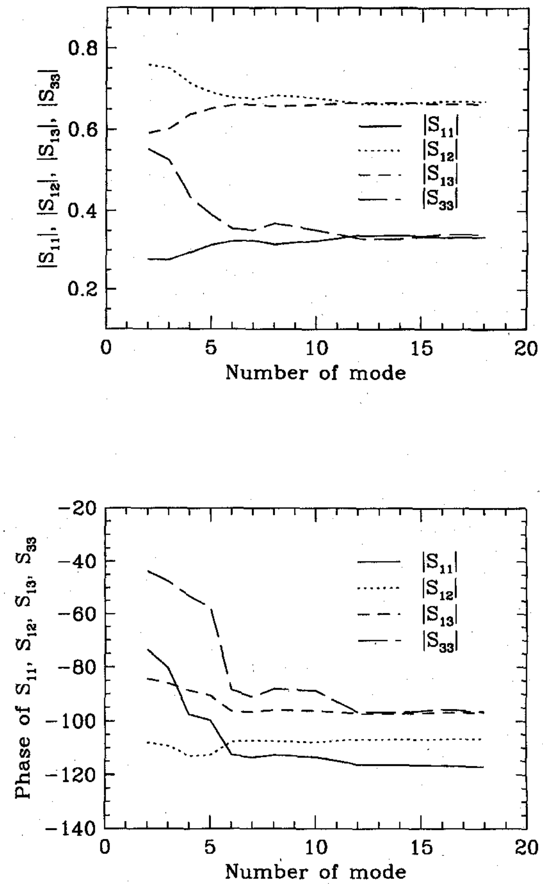

Fig. 8. Convergence of S-parameters of a double ridge waveguide T-junction at $f = 10\,\mathrm{GHz}$.T-junction dimensions $a_{1a} = a_{1b} = a_{1c} = 0.45''$, $a_{2a} = a_{2b} = a_{2c} = 0.34''$, $b_{1a} = b_{1b} = b_{1c} = 0.40''$, $b_{2a} = b_{2b} = b_{2c} = 0.15''$, $b_{3a} = b_{3b} = b_{3c} = 0.25''$, $b_{sa} = b_{sb} = 0.0''$.

By applying short condition at port 2, the reflection coefficients in the T-junction region can be obtained from (8b):

$$\begin{aligned}[b_i^T] &= \{[S_{11}^{i-2}] - [S_{12}^{i-2}][[U] \\ &\quad + [S_{22}^{i-2}]]^{-1}[S_{21}^{i-2}]\}[a_i^T] \\ &= [\Gamma_i][a_i^T].\end{aligned} \tag{9}$$

Substitute (9) into the two-port network S-parameters (8a), the field coefficients of incident and reflected waves $[a_i^T]$ and $[b_i^T]$

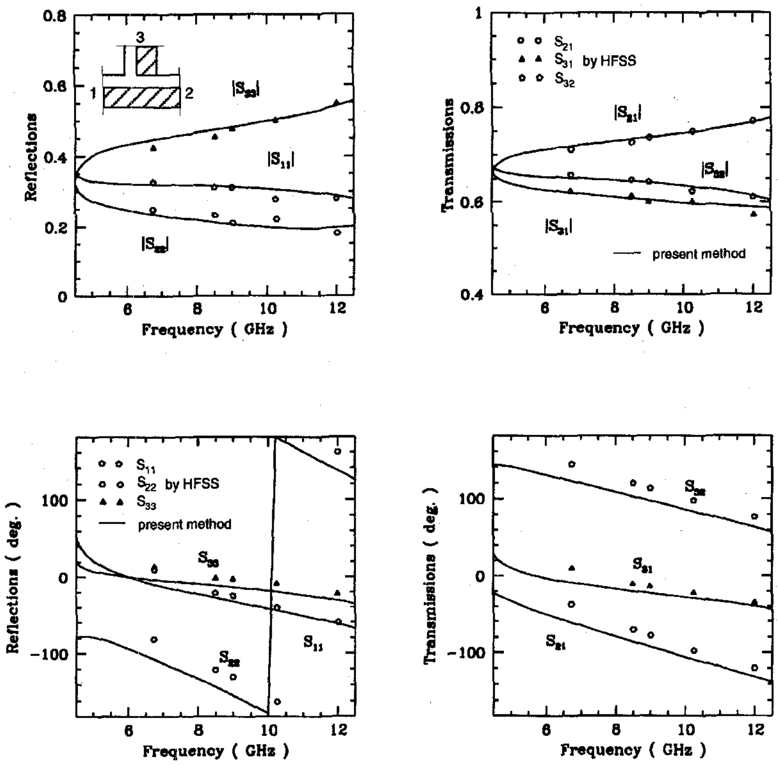

Fig. 9. S-parameters of a single ridge waveguide T-junction. T-junction dimensions $a_{1a} = a_{1b} = a_{1c} = 0.45''$, $a_{2a} = a_{2b} = a_{2c} = 0.34''$, $b_{1a} = b_{1b} = b_{1c} = 0.40''$, $b_{2a} = b_{2b} = b_{2c} = 0.0''$, $b_{3a} = b_{3b} = b_{3c} = 0.15''$, $b_{sa} = b_{sb} = 0.0''$.

in each region, in terms of the incident wave on port 1, can be obtained as

$$\begin{aligned}[a_i^T] &= [[U] - [S_{22}^{1-i}][\Gamma_i]]^{-1}[S_{21}^{1-i}][a_1] \\ &= [M_{ai}][a_1] \qquad (i = 1, 2, 3) \end{aligned} \tag{10a}$$

$$\begin{aligned}[b_i^T] &= [\Gamma_i][M_{ai}][a_1] \\ &= [M_{bi}][a_1] \qquad (i = 1, 2, 3). \end{aligned} \tag{10b}$$

By introducing inner products between the two sets of waveguide modes: one set in the subregion between ports 1 and 2, and the other in port 3, defined on the surfaces ΔS, as shown in Fig. 4(b), mode fields of the port 3 are expressed in terms of the field coefficients $[a^T{}_i]$, $[b^T{}_i]$ in the T-junction. This inner product is defined as

$$T_{mn}^{va} = \int_{\Delta S} \vec{h}_{tn}^{a} \cdot \vec{h}_{tm}^{v} \, ds \tag{11a}$$

$$T_{mn}^{vb} = \int_{\Delta S} \vec{h}_{tn}^{b} \cdot \vec{h}_{tm}^{v} \, ds \tag{11b}$$

where $\vec{h}_{tn}^{a}, \vec{h}_{tn}^{b}$ are the magnetic mode fields of the waveguide in the T-junction at the shorted vertical port 3, which are related to the field coefficients $[a_i^T]$ and $[b_i^T]$ in the T-junction, respectively; $\vec{h}_{tm}^{v}$ are the modal fields of the waveguide at port 3. In these inner products, all the integrands containing $e^{\pm\gamma z}$ terms should be integrated along the direction of which the wave moves, to preserve the accuracy and ensure the stability of the results.

The tangential magnetic fields at the shorted surface of port 3 is related to the incident fields as

$$[i_3] = \left\{ \sum_{i=1}^{3} \{[T_i^{va}][M_{ai}] - [T_i^{vb}][M_{bi}]\} \right\} [a_1]. \tag{12}$$

Thus the desired admittance matrix $[Y_{31}]$ can be obtained as

$$[Y_{31}] = \left\{ \sum_{i=1}^{3} \{[T_i^{va}][M_{ai}] - [T_i^{vb}][M_{bi}]\} \right\} [[U] + [\Gamma]]^{-1}. \tag{13}$$

Admittance matrix $[Y_{32}]$ can be computed in a similar way. The inner products defined in (11a) and (11b) for computing the admittance matrix $[Y_{31}]$ can also be used for computing $[Y_{32}]$, since only the field coefficients in the T-junction changed. As the power is flowing out of port 2, according to the defined coordinate system, negative sign should be added in the results.

C. Admittance Matrices $[Y_{33}]$, $[Y_{13}]$, and $[Y_{23}]$

Similar approach can be applied to obtain subadmittance matrices $[Y_{33}]$, $[Y_{13}]$, and $[Y_{23}]$ when field is incident from port 3 while ports 1 and 2 are shorted. Besides the discontinuity of ridge waveguide to ridge waveguide, generalized scattering matrices of ridge waveguide to empty waveguide, empty waveguide to bifurcated waveguide discontinuities have to be obtained in similar way as that of the ridge waveguide to ridge waveguide discontinuity. Applying the cascading procedure, the generalized scattering matrices of the imaginary two-port network from waveguide to bifurcated waveguide as shown in Fig. 5, can be obtained. Then applying short condition at the bifurcated waveguide side, the reflection coefficients $[\Gamma]$ can be obtained. Subadmittance matrix $[Y_{33}]$ is finally obtained from $[\Gamma]$ as

$$[Y_{33}] = [[U] - [\Gamma]][[U] + [\Gamma]]^{-1}. \tag{14}$$

Subadmittance matrices $[Y_{13}]$ and $[Y_{23}]$ can be obtained by reciprocity or following the same procedure as that of calculating the subadmittance matrices $[Y_{31}]$ and $[Y_{32}]$. According to the defined coordinate system, negative sign is needed for $[Y_{23}]$. When the ridge waveguide of port 2 has the same dimension as that of port 1, the calculation of the subadmittance matrices $[Y_{33}]$, $[Y_{13}]$, and $[Y_{23}]$ can be greatly simplified. The elements of the partial vertical inner products of T-junction to port 1 and 2, are positive or negative of those to ports 3 and 2.

IV. Results

Computer programs have been developed to obtain the eigenmodes of the double ridge waveguide, generalized scattering matrices of all the discontinuities needed and the generalized admittance matrix and S-matrix of the double ridge waveguide T-junctions in all three ports. The computed fields at the boundary of ridge waveguide's region I and II, and at the conducting surface of the ridge waveguide, shown in Fig. 6, ensure the correctness of the eigenmode's field coefficients. Fig. 7 shows the normalized dominant (TE) mode cutoff wavelength of a double-ridged waveguide with aspect ratio $b_1/a_1 = 0.5$. The results are in good agreement with [4].

Extensive convergence tests have been performed. Fig. 8 shows the convergence of the dominant mode's S-parameters for a double ridge waveguide T-junction at 10 GHz. Twelve modes are sufficient for convergence in most cases studied. The accuracy is within 1.0% for the magnitude and 2^o for the phase of the S-parameters. Since TM modes usually have higher cut-off frequency than TE modes, only about half the numbers of TM modes are needed to achieve the convergence. The method is so efficient that it only takes 7 s to obtain the generalized admittance and scattering matrices of a double ridge waveguide T-junction at one frequency point on the Sun Station 20 machine using 12 modes.

As a numerical example, the S-parameters of a single ridge waveguide T-junction over all frequency band are computed and the dominant mode's S-parameters are shown in Fig. 9. The T-junction has a 0.22″ wide and 0.25″ thick ridge in each arm with 0.90″ × 0.40″ cross section. This gives single mode operating bandwidth of 4.20 GHz to 12.53 GHz. Compared with the empty waveguide, ridge waveguide can reduce the size and increase the bandwidth of the system, but power handling of the device will decrease. The computed dominant mode's S-parameters of the T-junction are compared with the results obtained by the computer simulation software HFSS of Hewlett-Packard Company, which uses the finite element method. The results obtained by the two methods are in good agreement. It approximately takes 30 min, memory 60M bytes, on Sun Station 20 for HFSS to obtain only the dominant mode's S-parameters of the T-junction for a single frequency point. The present method is more than 200 times faster, and can run in the PC with 8M of RAM.

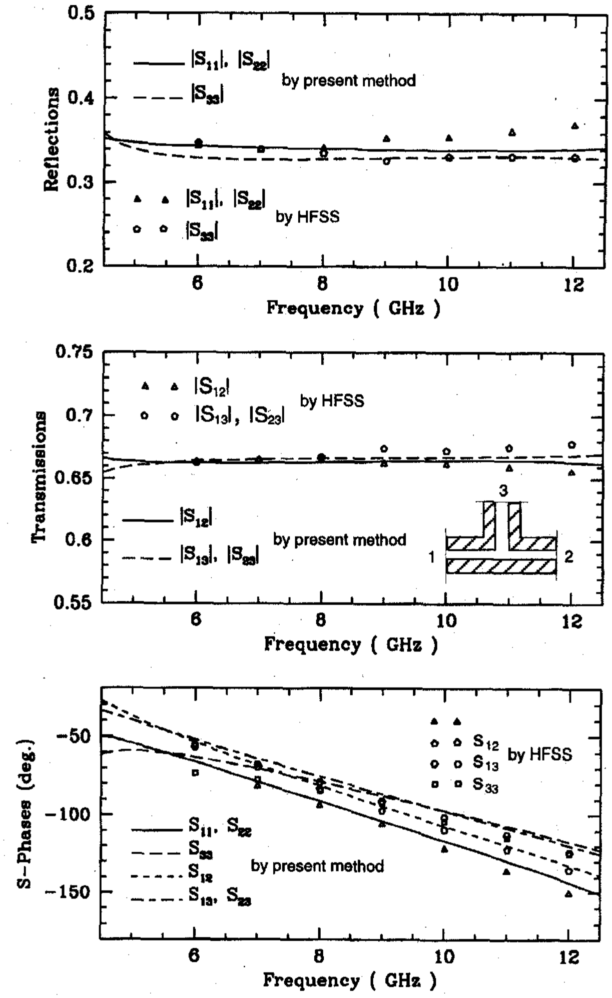

Fig. 10. S-parameters of a double ridge waveguide T-junction. T-junction dimensions $a_{1a} = a_{1b} = a_{1c} = 0.45''$, $a_{2a} = a_{2b} = a_{2c} = 0.34''$, $b_{1a} = b_{1b} = b_{1c} = 0.40''$, $b_{2a} = b_{2b} = b_{2c} = 0.15''$, $b_{3a} = b_{3b} = b_{3c} = 0.25''$, $b_{sa} = b_{sb} = 0.0''$.

Fig. 10 shows the computed dominant mode's S-parameters of a symmetrical double ridge waveguide T-junction. Using smaller gap between the double ridge, the T-junction gives wider single mode operation performance bandwidth than that of the previous example. It is seen that the magnitude of S-parameters of the double ridge waveguide T-junction is very flat over the whole frequency band, compared with that of the single ridge waveguide T-junction. The computed results of the double ridge waveguide T-junction are also compared with the results obtained by HFSS, and they are in good agreement.

V. Conclusion

A rigorous method for full wave modeling of the generalized double ridge waveguide T-junction has been developed. Based on the eigen mode expansion method and combining the cascading procedure and computation of the magnetic fields of each mode at the shorted ports from inner products and field coefficients, the generalized admittance and scattering matrices including all the higher order modes in all ridge waveguide ports are obtained. The method preserves numerical accuracy and accepts arbitrary cross section of all ports. The accuracy and versatility of the method are verified through several numerical examples. The computed dominant mode's S-parameters are compared with that by finite element method and shown to be in good agreement.

The method is general, very efficient, and can be used to solve other complicated multiport network problems.

Acknowledgment

The authors would like to thank Dr. A. S. Omar of Technische Universität Hamburg-Harburg, Germany, for his valuable suggestions and W. Luo who ran the computer simulation software HFSS of Hewlett-Packard Company to obtain the numerical results by finite element method.

References

[1] A. E. Atia, "Computer-aided design of waveguide multiplexers," *IEEE Trans. Microwave Theory Tech.,* vol. MTT-22, pp. 332–336, Mar. 1974.

[2] J. D. Rhodes and R. Levy, "Design of general manifold multiplexers," *IEEE Trans. Microwave Theory Tech.,* vol. 27, pp. 111–123, Feb. 1979.

[3] S. B. Cohn, "Properties of ridge wave guide," *Proc. IRE,* vol. 35, pp. 783–789, Aug. 1947.

[4] S. Hopfer, "The design of ridged waveguide," *IRE Trans. Microwave Theory Tech.,* vol. MTT-3, pp. 20–29, Oct. 1955.

[5] J. P. Montgomery, "On the complete eigenvalue solution of ridged waveguide," *IEEE Trans. Microwave Theory Tech.*, vol. MTT-19, pp. 547–555, June 1971.

[6] R. R. Mansour, R. S. K. Tong, and R. H. Macphie, "Simplified description of the field distribution in finlines and ridge waveguides and its application to the analysis of E-plane discontinuities," *IEEE Trans. Microwave Theory Tech.,* vol. 36, pp. 1825–1832, Dec. 1988.

[7] R. E. Collin, *Field Theory of Guided Waves.* New York: McGraw-Hill, 1960, pp. 103–113, 184–191.

[8] E. D. Sharp, "An exact calculation for a T-junction of rectangular waveguide having arbitrary cross sections," *IEEE Trans. Microwave Theory Tech.,* vol. MTT-15, pp. 109–116, Feb. 1967.

[9] F. Arndt, I. Ahrens, U. Papziner, U. Wiechmann, and R. Wilkeit, "Optimized E-plane T-junction series power dividers," *IEEE Trans. Microwave Theory Tech.,* vol. MTT-35, pp. 1052–1059, Nov. 1987.

[10] X.-P. Liang, K. A. Zaki, and A. E. Atia, "A rigorous three plane mode-matching technique for characterizing waveguide T-junctions, and its application in multiplexer design," *IEEE Trans. Microwave Theory Tech.,* vol. 39, pp. 2138–2147, Dec. 1991.

[11] H.-W. Yao, A. Abdelmonem, J.-F. Liang, X.-P. Liang, K. A. Zaki, and A. Martin, "Wide band waveguide and ridge waveguide T-junctions for diplexer applications," *IEEE Trans. Microwave Theory Tech.* vol. 41, pp. 2166–2173, Dec. 1993.

[12] A. Abdelmonem and K. A. Zaki, "Ridge waveguide T-junctions," in *IEEE MTT-S Dig.,* May 1995, pp. 757–760.

[13] Z. Ma and E. Yamsita, "Port Reflection coefficient method for solving Multiport Microwave Network Problems," *IEEE Trans. Microwave Theory Tech.,* vol. 43, pp. 331–337, Feb. 1995.

[14] H. W. Yao and K. A. Zaki, "Modeling generalized coaxial probes in rectangular waveguide," in *IEEE MTT-S Dig.,* May 1995, pp. 979–982.

[15] C. Wang, K. A. Zaki and R. Mansour, "Modeling of generalized double ridge waveguide T-junctions," in *IEEE MTT-S Dig.,* June 1996, pp. 1185–1188.

[16] A. S. Omar and K. Schünemann, "Transmission matrix representation of finline discontinuities," *IEEE Trans. Microwave Theory Tech.,* vol. MTT-33, pp. 765–770, Sept. 1985.

Chi Wang (S'96) was born in Zhe-Jiang, China, in 1961. He received the B.S. and M.S. degrees in electrical engineering from the Beijing Institute of Technology, Beijing, China, in 1983 and 1986, respectively.

He is now working toward the Ph.D. degree in electrical engineering at the University of Maryland at College Park. He was with the North China Vehicle Research Institute in 1986. During 1992–1993 was a Research Associate at the Beijing Institute of Technology. His research interests are in the modeling and design of microwave waveguide devices and circuits.

Kawthar A. Zaki (SM'85–F'91) received the B.S. degree with honors from Ain Shams University, Cairo, Egypt, in 1962 and the M.S. and Ph.D. degrees from the University of California, Berkeley, in 1966 and 1969, respectively, all in electrical engineering.

From 1962 to 1964, she was a Lecturer with the Department of Electrical Engineering, Ain Shams University. From 1965 to 1969, she held the position of Research Assistant with the Electronic Research Laboratory, University of California, Berkeley. She joined the Electrical Engineering Department, University of Maryland, College Park, in 1970, where she is presently Professor of electrical engineering. Her research interests are in the areas of electromagnetics, microwave circuits, optimization, computer-aided design, and optically controlled microwave and millimeter wave devices.